18th Brazilian Congress of Thermal Sciences and Engineering
November 16-20, 2020 (Online)

ENC-2020-0054
GEOMETRICAL EVALUATION OF A SEABED STRUCTURE COUPLED WITH AN ONSHORE OVERTOPPING WAVE ENERGY CONVERTER APPLYING CONSTRUCTAL DESIGN

Andréia Sá de Barros
Danyllo de Moura Amaral
Liércio André Isoldi
Graduate Program of Ocean Engineering, Universidade Federal do Rio Grande - FURG, Italia Avenue, km 8, 96201-900, Brazil
a.sadebarros@gmail.com, danylloway@gmail.com, liercioisoldi@furg.br

Luiz Alberto Oliveira Rocha
Mechanical Engineering Graduate Program, Universidade do Vale do Rio dos Sinos – UNISINOS, São Leopoldo, 93022-750, Brazil
luizor@unisinos.br

Mateus das Neves Gomes
Instituto Federal de Educação, Ciência e Tecnologia do Paraná - IFPR, Antônio Carlos Rodrigues Street, 453, Paranaguá, 83215-750, Brazil
mateus.gomes@ifpr.edu.br

Elizaldo Domingues dos Santos
Graduate Program of Ocean Engineering, Universidade Federal do Rio Grande - FURG, Italia Avenue, km 8, 96201-900, Brazil
elizaldosantos@furg.br

Abstract. *Present numerical work performs the geometrical evaluation of an overtopping wave energy conversion with a coupled structure (rectangular obstacle) mounted on the seabed of a real scale wave tank by means of Constructal Design. It is simulated the main operational principle of device. The main purpose here is to evaluate the design of the overtopping that maximizes the water accumulated into reservoir. The problem studied has been subject to three constraint areas (tank, overtopping ramp and seabed placed rectangular obstacle) and two degrees of freedom: height/length ratio of the ramp (H_3/L_3) (or ramp slope) and distance between the bottom of wave tank and the device (H_1). Conservation equations of mass, momentum and one transport equation for volume fraction of water are solved with the finite volume method. To tackle with water-air mixture, multiphase model Volume of Fluid is used. Results indicated that the variation in the obstacle height (H_1) influenced the effect of the ratio H_3/L_3 over the mass accumulated in the reservoir, as well as, change the optimal configuration of the ramp. The insertion of rectangular obstacle reduced in almost 9 times the mass of water accumulated in the reservoir in comparison with a case without obstacle.*

Keywords: *Constructal Design, Numerical Simulation, Geometric Evaluation, Overtopping Device, Wave Energy Converter.*

1. INTRODUCTION

Present study is concerned with geometrical assessment of an overtopping wave energy converter (OWEC). Its main operational principle consists on the water accumulation into a reservoir raised above the sea level. The water overtops the inclined ramp and enters into the reservoir. The accumulated water returns to the sea passing through low head hydraulic turbines generating electricity (Kofoed *et al*., 2006).

Several contributions about the design of OWECs have been presented in literature (Kofoed *et al*., 2006; Victor *et al.*, 2011; Musa *et al.*, 2017). In spite of important contributions, few works have been performed using Constructal Design, which is a method for prediction of design of any finite size flow system based in a physical principle (Constructal Law of design and evolution) of maximization of access to its internal currents (Bejan, 2000; Bejan and Lorente, 2008, Bejan, 2016).

Among the few contributions into Constructal Design framework for geometrical evaluation of OWECs, it is possible to mention the work of Dos Santos *et al*., (2014), which determine the influence of geometry on the performance of an offshore overtopping device in laboratory scale to three different relative depths (h/λ = 0.3, 0.5 and 0.62). Results showed that the optimal ratio between height and length of the ramp, $(H_1/L_1)_o$, had a strong dependence of the relative depth,

indicating the absence of a best universal geometry. Afterwards, Goulart *et al.*, (2015) performed a two-dimensional numerical study about the effect of the ramp geometry on the performance of a nearshore overtopping device in real scale employing Constructal Design. It was investigated the effect of height to length ratio of the ramp (H_1/L_1) over the mass of water (m) entering in the reservoir along a time interval of t_f = 100.0 s for two different depths (S = 5.0 m and 6.0 m). For all cases, it is considered a construction area for the ramp (φ = 0.012) and subjected to a monochromatic wave with T = 7.5 s and H = 1.0 m. Results obtained in this work led to different effect of the ratio H_1/L_1 over the mass that overtops the device in comparison with previous work of Dos Santos *et al.* (2014). Afterwards, Martins *et al.* (2018) extrapolated the studied performed in Goulart et al. (2015) for different magnitudes of ramp area ($0.006 \leq \varphi \leq 0.024$) and different submergences (S) of device. Important recommendations about the design were achieved, e.g., results showed for fixed magnitudes of submergence that the best performance was reached for the lowest magnitudes of ramp slope. Moreover, for some fractions of area, intermediate submergences led to the best performance. In the three works, a computational model based on the FVM and VOF was employed to tackle with water/air multiphase flow. In the present work, it is investigated the influence of a rectangular seabed structure coupled with the ramp over the performance of the device.

Present numerical work has the purpose to evaluate the geometry by means of Constructal Design associated with Exhaustive Search of an onshore OWEC coupled with a rectangular obstacle placed in the seabed of a wave tank in real scale. It is considered a two-dimensional tank with an onshore OWEC subjected to the incidence of monochromatic waves. Here, it is evaluated the distance between the bottom of wave tank and the device (H_1) and the ratio between the height and length of ramp (H_3/L_3), over the mass of water that overtops the ramp.

2. MATHEMATICAL AND NUMERICAL MODELING

The physical problem consists on a two-dimensional wave tank with an onshore OWEC coupled with a rectangular obstacle placed in the seabed, as can be seen in Fig. 1. Concerning the problem dimensions, it is considered a water layer of h = 10 m, height and length of wave tank of H_T = 20 m and L_T = 320 m. The oncoming monochromatic wave has a wavelength of λ = 65.4 m, a period of T = 7.5 s and height of H = 1.0 m. For the initial condition, the fluid is at rest.

Concerning the boundary conditions, the wave is generated by an imposition of velocity field in the left surface of the channel (red lines in Fig. 1), mimicking a wavemaker. For the other boundary conditions, the superior region of left side surface and the superior surface are considered at atmospheric pressure P_g = 0 atm (blue lines in Fig. 1). In the lower and right surfaces, as well as, in the overtopping device surfaces (green and pink lines in Fig. 1) it is imposed a non-slip condition and impermeability ($u = w$ = 0 m/s). Regarding the initial conditions, it is considered that the fluid is at rest and the depth of water layer is h = 10.0 m. The device is considered fixed for each magnitude of H_1 studied in the present work.

For geometrical evaluation, the problem has three constraints: total area of wave tank (A_T), fraction area of the ramp given by the ratio between the ramp area (A_r) and total area of the tank ($\varphi = A_r/A_T$ = 0.012) and fraction area of the obstacle placed given by the ratio between obstacle area (A_t) and total area of the tank ($\varphi_1 = A_t/A_T$ = 0.006). Moreover, the following degrees of freedom are defined: H_T/L_T, H_3/L_3 and H_1 (submergence). In the present work the ratio H_3/L_3 is varied for two different magnitudes of H_1, while H_T/L_T is kept constant. There is also a geometric constraint so that the wave crest does not exceed the height of the device, thus preventing overtopping, so it is necessary that $(H_1+H_3) > (h + H/2)$.

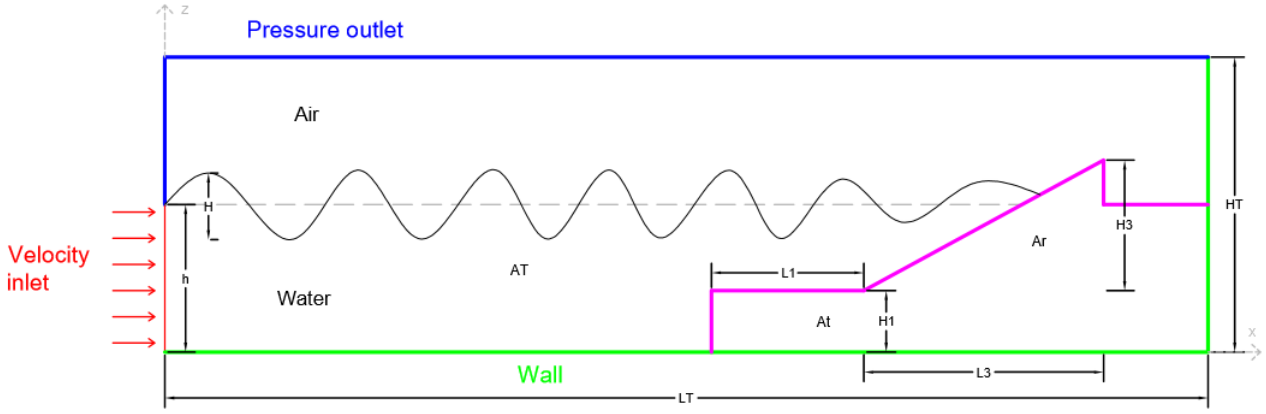

Figure 1 – Computational domain of wave tank with overtopping device and rectangular obstacle.

According to Constructal Design, the geometric evaluation is subjected to three constraints, these being, the total area of wave tank,

$$A_T = H_T L_T \tag{1}$$

the area of the ramp,

$$A_r = \frac{H_3 L_3}{2} \tag{2}$$

and the area of the rectangular obstacle.

$$A_t = H_1 L_1 \tag{3}$$

The area of the ramp and obstacle can be represented by area fractions defined as:

$$\varphi = \frac{A_r}{A_T} \tag{4}$$

$$\varphi_1 = \frac{A_t}{A_T} \tag{5}$$

The main purpose is to maximize the amount of mass that overtops the device. Therefore, it is monitored the mass flow rate that overtops the ramp at each instant of time and accumulates in the reservoir. From the mass flow rates ($\dot{m}$) as function of time, it is possible to determine the total amount of mass of water that enters in the reservoir by:

$$m = \frac{1}{t_f}\int_0^{t_f} \dot{m}\, dt \tag{6}$$

where t_f is the period of time of the studied problem (s) and $\dot{m}$ is the mass flow rate (kg/s). For all studied cases, it is considered a period of t_f = 100.0 s.

The optimization process consists on the association between Constructal Design and Exhaustive Search, where the former is used to define the search space and the performance indicators and the latter is responsible for sweeping of the search space. Figure 2 illustrates the flowchart of the simulated cases in the present work. The first step consists on the variation of the ratio H_3/L_3 for constant values of H_1 = 3.0 m and φ = 0.012. The highest magnitude of mass of water (m) that enters in the reservoir is the once maximized mass of water, m_m, and the corresponding optimal ratio of H_3/L_3 is the once optimized ratio H_3/L_3, $(H_3/L_3)_o$. The second step consists on the repetition of step one for other magnitudes of H_1, founding the twice maximized mass of water entering in the reservoir, m_{mm}, and the corresponding optimal degrees of freedom: once optimized magnitude of H_1, $(H_1)_o$ and the twice optimized ratio of H_3/L_3, $(H_3/L_3)_{oo}$. Here, only two different magnitudes of H_1 are investigated due to the high computational effort for each simulation. It is also worthy to mention that, changes in the magnitude of H_1 can led to modifications in the range of possible geometries represented by the ratios of H_3/L_3 studied.

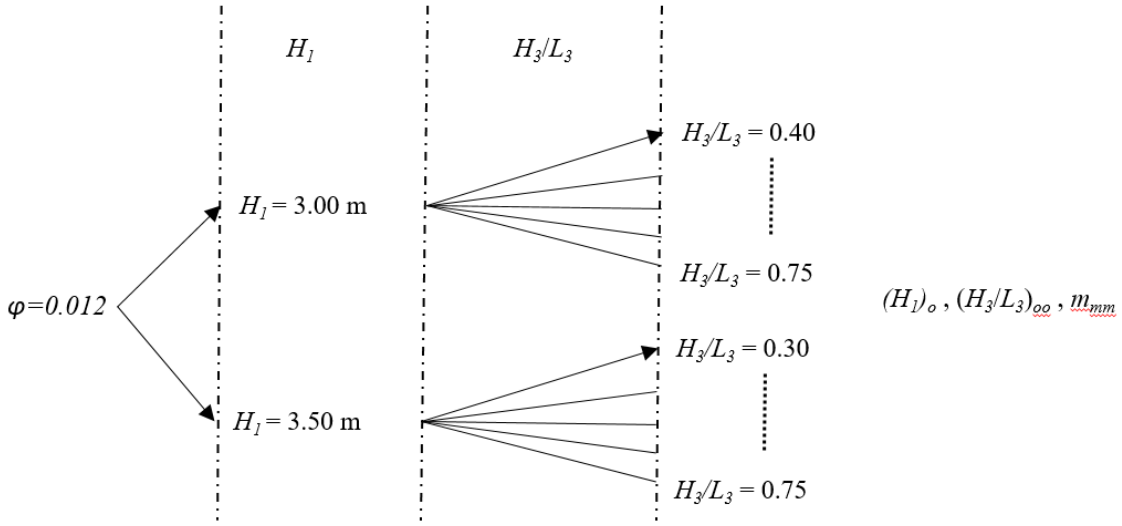

Figure 2 – Flowchart of performed simulations in the geometric evaluation of the studied overtopping device.

The incompressible, isothermal, laminar and incompressible multiphase flow of air/water mixture is modeled with the conservation equations of mass, momentum and one equation for volume fraction of water (Schlichting, 1979; Hirt and Nicholz, 1981; Lv et al., 2011).

The conservation equation of mass for the mixture air/water is given by:

$$\frac{\partial \rho}{\partial t} + \nabla.(\rho \vec{v}) = 0 \tag{7}$$

where ρ is the density of the mixture (kg/m^3) and $\vec{v}$ is the flow velocity vector (m/s).

Momentum equation for the mixture is given by:

$$\frac{\partial}{\partial t}(\rho \vec{v}) + \nabla.(\rho \vec{v}\vec{v}) = -\nabla p + \nabla.(\bar{\bar{\tau}}) + \rho \vec{g} \tag{8}$$

where p is the pressure (N/m^2), $\rho \vec{g}$ is the buoyancy forces (N/m^3) and $\bar{\bar{\tau}}$ is the stress deformation tensor (N/m^2). Values of air and water properties are given respectively by: ρ_{air} = 1.225 kg/m^3, ρ_{water} = 998.200 kg/m^3, μ_{air} = 1.789 × 10^{-5} kg/(ms), μ_{water} = 1.003 × 10^{-3} kg/(ms).

To tackle with the interface water/air it is employed the Volume of Fluid (VOF) method (Hirt and Nichols, 1981). Therefore, the concept of volume fraction (α_q) is used to represent the two phases in a control volume. In this model, the sum of the volume fractions within a control volume must be unitary ($0 \leq \alpha_q \leq 1$). Consequently, if $\alpha_{water} = 0$, the control volume is empty of water and full of air ($\alpha_{air} = 1$). If the fluid is a mixture of air and water, one phase is the complement of the other, $\alpha_{air} = 1 - \alpha_{water}$. Thus, only one additional transport equation for the volume fraction is required (Hirt *et al*., 1981; Lv *et al*., 2011):

$$\frac{\partial(\alpha_{water})}{\partial t} + \nabla.(\vec{v}\alpha_{water}) = 0 \tag{9}$$

Conservation equations of mass and momentum are solved for the mixture. Therefore, it is necessary to obtain density and viscosity values for the mixture, which can be written, respectively, by:

$$\rho = \alpha_{água}\rho_{água} + \alpha_{ar}\rho_{ar} \tag{10}$$

$$\mu = \alpha_{água}\mu_{água} + \alpha_{ar}\mu_{ar} \tag{11}$$

Regarding the wave generation, a velocity profile is imposed at the left side surface of the wave tank (see red line in Fig. 1), simulating the behavior of a wavemaker (Horko,2007). Velocity components in the wave propagation (x) and vertical (z) directions imposed in the left surface of the domain are based on Stokes 2nd order wave theory and given, respectively, by (Chakrabarti, 2005):

$$u(x,z) = \frac{Hgk}{2\sigma}\frac{\cosh k(h+z)}{\cosh(kh)}\cos(kx-\sigma t) + \frac{3H^2\sigma k}{16}\frac{\cosh 2k(h+z)}{\sinh^4 kh}\cos 2(kx-\sigma t) \tag{12}$$

$$w(x,z) = \frac{Hgk}{2\sigma}\frac{\sinh k(h+z)}{\cosh(kh)}\sin(kx-\sigma t) + \frac{3H^2\sigma k}{16}\frac{\sinh 2k(h+z)}{\sinh^4 kh}\sin 2(kx-\sigma t) \tag{13}$$

where H is the wave height (m), h is the water depth (m), T is the wave period (s) and t is the time (s).

For each geometrical configuration, the conservation equations of mass and momentum for mixture of water/air and one transport equation of volumetric fraction of water are solved with the Finite Volume Method (FVM) (Patankar, 1980). More precisely, it is employed the Software FLUENT, version 14 (FLUENT, 2013). The solver is pressure based and PISO method is used for coupling pressure-velocity. Concerning the solution of advection terms, it is employed Upwind scheme and Geo-reconstruction method is used for reconstruction of volume fraction.

The solution is considered converged when the residuals of all equations are lower than 10^{-6}. Discretization of the computational domain is performed with rectangular finite volumes, as can be seen in Fig. 3. The highest refinement is performed in device surfaces and wave free surface, i.e., the regions where the highest velocity gradients are noticed. In the study of Gomes *et al.* (2012) it is presented a theoretical recommendation about the number of finite elements employed along the domain, mainly in the wave length and height directions, which is adopted in the present study. In this sense, a grid with nearly 92,800 rectangular finite volumes is generated. Moreover, a time-step of Δt = 0.05 s is employed in all simulations. It is worthy to mention that the values employed for spatial and time-discretization are similar to that employed in the works of Goulart *et al.* (2015) and Martins *et al.* (2018) for an overtopping without seabed obstacle.

All simulations are performed using a computer with two dual- core Intel Core processors i7-4960X 3.60 GHz and 32 GB of RAM. The processing time for each simulation is approximately 2.88×10^4 s (8 h).

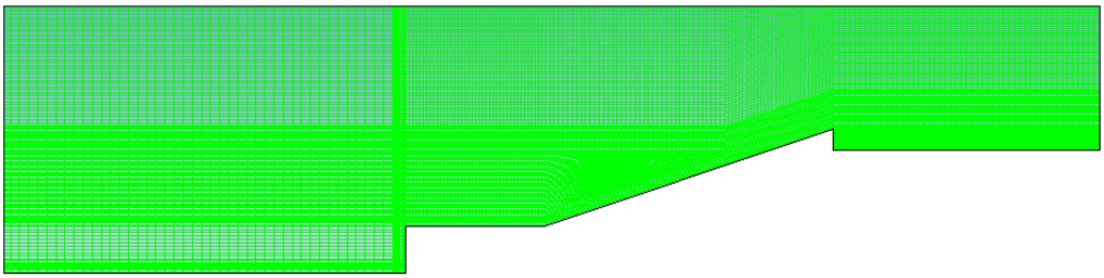

Figure 3 – Spatial discretization of the computational domain for the numerical simulation of the overtopping device.

3. RESULTS AND DISCUSSION

In the present study, two different magnitudes of H_1 are investigated (H_1 = 3.0 m and 3.5 m). Firstly, it is obtained the behavior of the mass flow rate of water that enters in the device reservoir as a function of time. For H_1 = 3.0 m the ratio H_3/L_3 is investigated in the range ($0.4 \leq H_3/L_3 \leq 0.75$). Figure 3 shows the instantaneous mass flow rate for three different ratios of H_3/L_3 when H_1 = 3.0 m. As can be noticed, there is only few occurrences of overtopping in the device for the different ratios of H_3/L_3 investigated. For H_3/L_3 = 0.4 (the lowest magnitude possible for H_1 = 3.0 m) only two peaks of mass flow rate are noticed for the instants of time t = 57.0 s and 65.5 s, where the first peaks are noticed. For H_3/L_3 = 0.45 four peaks are noticed with higher intensity and when H_3/L_3 = 0.5 there is no more overtopping. Concerning the highest magnitudes of mass flow rate, when H_3/L_3 = 0.45 it is achieved magnitudes of almost 1,400 kg/s of mass flow rate, while for H_3/L_3 = 0.4, the highest magnitude decreases to nearly 800 kg/s. In general, results indicated that the extreme inferior ratio of H_3/L_3 is not the best configuration, different from previous observations of Goulart et al. (2015) and Martins et al. (2018) for the overtopping without seabed obstacle, which achieved the optimal configurations for the lowest possible magnitudes of H_3/L_3. When present results are compared with those found in Goulart *et al.* (2015) and Martins *et al.* (2018) for the same fluid dynamic and geometry conditions, it is possible to observe that the insertion of the obstacle smoothed the time interval of each occurrence of overtopping, as well as, the number of occurrences for the same period of analysis (t_f = 100.0 s).

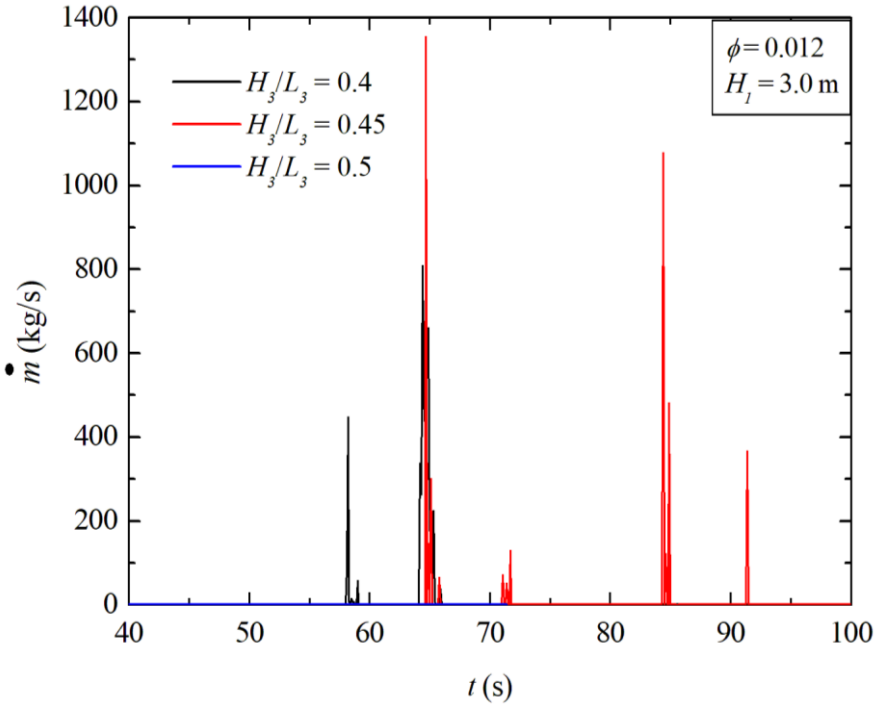

Figure 4 – Mass flow rate as function of time for different ratios H_3/L_3 and H_1 = 3.0 m.

For the case with H_1 = 3.5 m, the range of the studied ratios of H_3/L_3 changed for $0.3 \leq H_3/L_3 \leq 0.75$. It is worthy to mention that for H_1 = 3.0 m due to the restriction of height of ramp and device, $(H_1+H_3) > (h + H/2)$, it is impossible to generate configurations with $H_3/L_3 < 0.4$ for the previous case. Figure 5 shows the instantaneous mass flow rates for the case with H_1 = 3.5 m and three different magnitudes of H_3/L_3 (H_3/L_3 = 0.3, 0.35 and 0.4). In spite of the achievement of lower magnitudes for each peak of overtopping, the number of occurrences and the time interval of each occurrence increases, which can led to a higher amount of water entering in the reservoir in comparison with the cases with H_1 = 3.0 m. In this case, only the accounting of the total amount of mass can supply an adequate comparison. Among the three compared ratios of H_3/L_3, it seems that the intermediate ratio of H_3/L_3 = 0.35 led to the best performance for H_1 = 3.5 m.

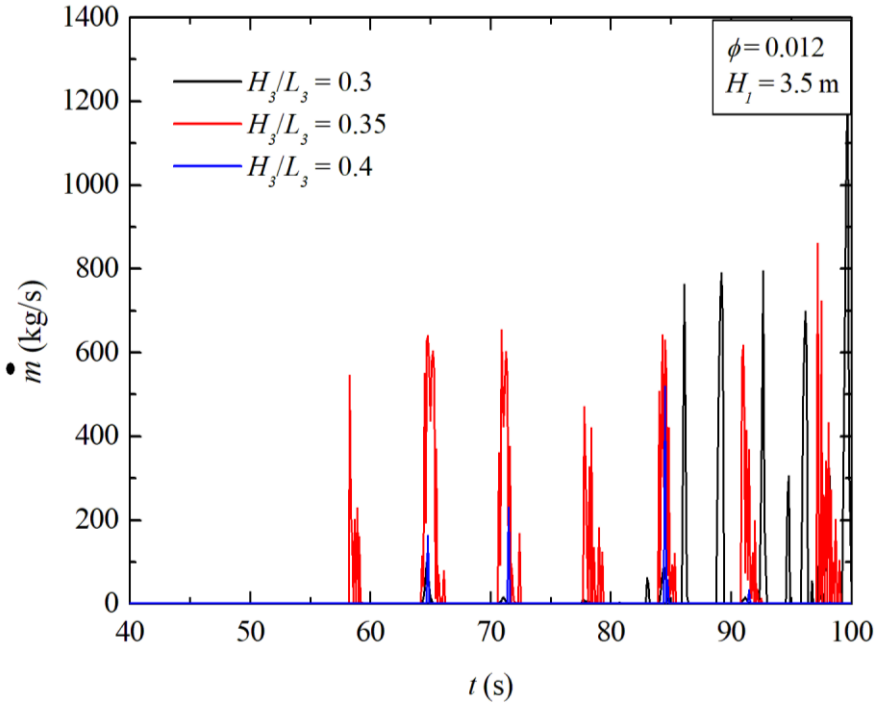

Figure 5 – Mass flow rate as function of time for different ratios H_3/L_3 and H_1 = 3.5 m.

Figure 6 shows the effect of the ratio H_3/L_3 over the total amount of water that overtops the ramp and enters the reservoir. The accounting of the total mass entering in the reservoir consists on the employment of Eq. (6) along the time interval of t_f = 100.0 s. Results indicated that the best shapes are achieved for intermediate ratios of H_3/L_3, i.e., intermediate slopes of the ramp. This behavior is different to previous findings of Goulart *et al.* (2015) and Martins *et al.* (2018) which simulated real scale overtopping devices without the seabed obstacles. However, the behavior is similar to the results reached by Dos Santos *et al.* (2014) for overtopping device placed in a laboratory scale wave tank. The behavior of H_3/L_3 over m obtained here can be associated with wave flows reaching the ramp with low intensity. In the present simulations, this decrease of flow intensity can be associated with the reflection and refraction effects imposed by the insertion of rectangular obstacle. In spite of change of the optimal ratio from the lowest extreme ratio of H_3/L_3 to an intermediate ratio, for all cases, the highest magnitudes of the ratios H_3/L_3 led to the worst performance, as expected. The comparison between two different magnitudes of H_1 also indicated that the highest submergence of the ramp was beneficial in the present configuration. The best shape reached for H_1 = 3.0 m is almost 30% better than the best configuration found for H_1 = 3.5 m.

For the same fluid dynamic conditions, a comparison between the best cases with rectangular obstacle and cases without obstacle studied in the works of Goulart *et al.* (2015) and Martins *et al.* (2018) is performed. The best shape found here led to an amount of accumulated water of m = 1,150 kg, while the best performance reached for cases without ramp is nearly m = 10,000 kg, i.e., almost nine (9) times inferior. Therefore, results indicated that rectangular obstacles placed in the seabed of the tank are recommended as a breakwater, not for wave energy conversion purposes. Probably, the employment of obstacles placed in the seabed with low reflective and refractive behavior can improve the performance of the system in comparison with cases without obstacle, working well for wave energy conversion purposes. In this sense, studies about the influence of triangular and trapezoidal obstacles in the mass of water entering in the device are recommended.

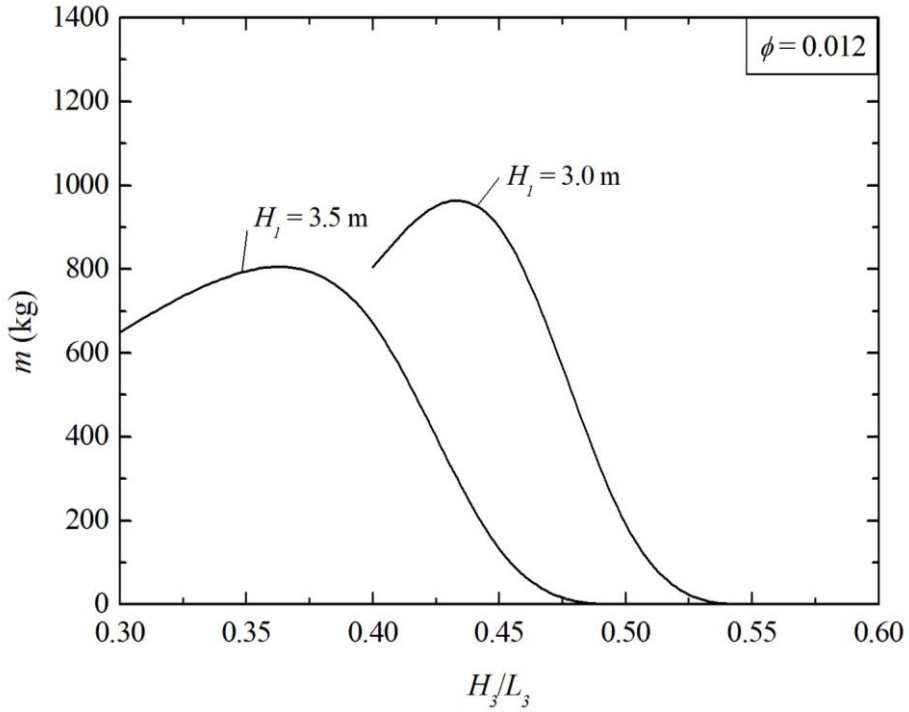

Figure 6 – Effect of the ratio H_3/L_3 over the mass of water (m) that enters in the overtopping reservoir.

4. CONCLUSIONS

The present numerical work performed a geometrical investigation of an onshore overtopping wave energy conversion with a coupled structure of rectangular shape mounted in the seabed of a real scale wave tank. Constructal Design was employed for definition of search space of geometric configurations and performance indicator. Moreover, Exhaustive Search was used to sweeping the cases of investigation. Conservation equations of mass, momentum and one equation for transport of volume fraction were solved numerically with the Finite Volume Method (FVM).

In general, results indicated that the use of rectangular obstacle in the seabed was not recommended to improve the performance of wave energy conversion. The best shape reached here (H_1 = 3.0 m and H_3/L_3 = 0.44) led to a performance almost nine (9) times inferior than similar cases without the use of obstacle, studied in the works of Goulart *et al.* (2015) and Martins *et al.* (2018). Therefore, this kind of structure is more recommended for port defense structures.

Results also indicated that the effect of the ramp over the mass of water that enter in the reservoir changed significantly in comparison with the cases without obstacles previously studied in the literature for real scale onshore overtopping devices, see the works of Goulart *et al.* (2015) and Martins *et al.* (2018). Here, intermediate optimal slopes for the ramp were achieved, which is a behavior similar to that found in Dos Santos *et al.* (2014) for overtopping devices subject to waves with low intensity simulated in laboratory scale. Therefore, results indicated that this effect can be a characteristic behavior of the effect of ramp over the mass of water that enters in the reservoir for wave systems of low intensity. The achievement of optimal shapes with the lowest ratios of ramp slope and decrease of *m* with the augmentation of H_3/L_3 can represent the behavior of systems with high intensity. Future investigations should be performed to corroborate these findings.

As future studies, the insertion of other shapes for the obstacles as triangular and trapezoidal are recommended to observe their influence over the performance of the wave energy converter. These investigations are in progress.

5. ACKNOWLEDGEMENTS

A. S. de Barros thanks CAPES (Coordination for the Improvement of Higher Educational Personal – Brasília, DF, Brasil) for Master Science Scholarship (Finance Code 001). D. M. Amaral thanks CNPq (National Counsel of Technological and Scientific Development – Brasília, DF, Brazil) for Scientific Iniciation scholarship. L. A. Isoldi, L.A.O. Rocha and E.D. dos Santos thank CNPq for research grants (Process: 306012/2017-0, 306024/2017-9 and 307847/2015-2). All authors thank CNPq for financial support in the project of CNPq/Equinor Ltda Call Nº 38/2018 (Process: 440010/2019-5).

6. REFERENCES

Bejan, A. and Lorente, S., 2008. *Design with constructal theory*. John Wiley & Sons, Hoboken, New Jersey, USA.

Bejan, A., 2000. *Shape and structure, from engineering to nature*. Cambridge University Press, New York, USA.

Bejan, A., 2016. *The physics of life: the evolution of everything*. St. Martins Press, New York, USA.

Chakrabarti, S.K. 2005. *Handbook of Offshore Engineering*, Elsevier, Amsterdam, Netherlands.

Dos Santos, E.D., Machado, B.N., Zanela, M.N., Gomes, M. das N., Souza, J.A., Isoldi, L.A. and Rocha, L.A.O., 2014. "Numerical Study of the effect of the relative depth on the overtopping wave energy converters according to Constructal Design". *Defect and Diffusion Forum*, Vol. 348, pp. 232 – 244.

FLUENT, 2013. *Documentation Manual* – FLUENT 14.3.

Gomes, M. das N., Dos Santos, E.D., Isoldi, L.A. and Rocha, L.A.O. 2012. "Grid analysis for numerical generation of waves in tanks (in Portuguese)", in: *Proceedings of VII National Congress of Mechanical Engineering*, São Luiz; Maranhão, Brazil.

Goulart, M.M., Martins, J.C., Acunha Jr, I.C., Gomes, M. das N., Souza, J.A., Rocha, L.A.O., Isoldi, L.A. and Dos Santos, E.D., 2015. "Constructal Design of an onshore overtopping device in real scale for two different depths". *Marine System and Ocean Technolology*, Vol. 10, pp. 120 – 129.

Hirt, C.W. and Nichols, B.D. 1981. Volume of fluid (VOF) method for the dynamics of free boundaries, *Journal of Computational Physics*, Vol. 39, pp. 201 - 225.

Horko, M. 2007. *CFD Optimization of an Oscillating Water Column Energy Converter*, Master Dissertation Thesis, The University of Western.

Kofoed, J.P., Frigaard, P., Friis-Madsen, E. and Sørensen, H.C., 2006. "Prototype testing of the wave energy converter wave dragon", *Renewable Energy*, Vol. 31, pp. 181 – 189.

Lv, X., Zou, Q. and Reeve, D., 2011. "Numerical simulation of overflow at vertical weirs using a hybrid level set/VOF method", *Advances in Water Resources*, Vol. 34, pp. 1320 – 1334.

Martins, J.C., Goulart, M.M., Gomes, M. das N., Souza, J.A., Rocha, L.A.O., Isoldi, L.A. and dos Santos, E.D., 2018. "Geometric evaluation of the main operational principle of an overtopping wave energy converter by means of Constructal Design". *Renewable Energy*, Vol. 118, pp. 727 – 741.

Musa, M.A., Maliki, A.Y., Ahmad, M.F., Sani, W.N., Yaakob, O. and Samo, K.N., 2017. "Numerical simulation of wave flow over the overtopping breakwater for energy conversion (OBREC) device", *Procedia Engineering*, Vol. 194, pp. 166 – 173.

Patankar, S.V., 1980. *Numerical Heat Transfer and Fluid Flow*. McGraw-Hill, New York, USA.

Schlichting, H., 1979. *Boundary Layer Theory.* Seventh Ed. McGraw-Hill, New York, USA.

Victor, L., Troch, P., and Kofoed, J.P., 2011. "On the effects of geometry control on the performance of overtopping wave energy converters", *Energies*, Vol. 4, pp. 1574 – 1600.

7. RESPONSIBILITY NOTICE

The authors are the only responsible for the printed material included in this paper.